

Pressure dependence of the Curie temperature in Ni₂MnSn Heusler alloy: A first-principles study

E. Şaşıoğlu, L. M. Sandratskii and P. Bruno

Max-Planck Institut für Mikrostrukturphysik, D-06120 Halle, Germany

(Dated: October 20, 2018)

The pressure dependence of electronic structure, exchange interactions and Curie temperature in ferromagnetic Heusler alloy Ni₂MnSn has been studied theoretically within the framework of the density-functional theory. The calculation of the exchange parameters is based on the frozen-magnon approach. The Curie temperature, T_c , is calculated within the mean-field approximation by solving the matrix equation for a multi-sublattice system. In agreement with experiment the Curie temperature increased from 362K at ambient pressure to 396 at 12 GPa. Extending the variation of the lattice parameter beyond the range studied experimentally we obtained non-monotonous pressure dependence of the Curie temperature and metamagnetic transition. We relate the theoretical dependence of T_c on the lattice constant to the corresponding dependence predicted by the empirical interaction curve. The Mn-Ni atomic interchange observed experimentally is simulated to study its influence on the Curie temperature.

PACS numbers: 75.50.Cc, 75.30.Et, 71.15.Mb, 74.62.Fj

I. INTRODUCTION

The pressure dependence of the Curie temperature provides important information on a ferromagnetic system and is an object of intensive studies both experimental^{1,2,3,4} and theoretical.^{5,6,7,8,9,10} The key question here is the character of the variation of various magnetic properties with decreasing distances between magnetic atoms. In an early work, Castellitz¹¹ proposed an empirical rule (interaction curve) that describes the dependence of the Curie temperature of the Mn-containing ferromagnetic alloys with 4-5 valence electrons per molecule on the ratio R/d where R is the nearest-neighbor Mn-Mn distance and d is the radius of the atomic Mn 3d shell. The curve is supposed to represent the Curie temperatures of various systems at ambient pressure as well as the pressure dependence of T_c of a given system. The function is not monotonous and has a maximum at the R/d value of about 3.6 (see Fig. 8). According to the interaction curve, one can expect $dT_c/dP > 0$ for alloys with $R/d > 3.6$ (e.g., Ni₂MnSn and Cu₂MnIn). On the other hand, the systems with $R/d < 3.6$ (e.g., NiAs-type MnAs, MnSb and MnBi) are expected to have negative pressure dependence of the Curie temperature. These predictions are in agreement with experiment.^{12,13,14}

Recently Kanomata *et al.* suggested a generalization of the interaction curve to the case of 6-7 valence electrons per chemical formula.¹⁵ These systems form a new branch of the dependence of the Curie temperature on the Mn-Mn distance (Fig. 8). The available experimental values of the pressure derivative of the Curie temperature, dT_c/dP , for Heusler alloys are consistent with those expected from the interaction curve.^{16,17,18}

Early experiments on the pressure dependence of the Curie temperature of Heusler alloys have been performed in a low pressure region (less than 0.5 GPa). Recently Gavriluk *et al.*¹⁹ have studied structural and magnetic

properties of Ni₂MnSn in the pressure interval up to 10.8 GPa. The authors have found an increasing linear dependence of the Curie temperature on applied pressure. The Mössbauer spectroscopy revealed partial interchange of the Mn and Ni atoms.

The purpose of the present work is a first-principles study of the electronic structure, exchange interactions and Curie temperature in Ni₂MnSn as a function of pressure. The main attention is devoted to the interval of the interatomic Mn-Mn distances from 4.26Å to 4.06Å that corresponds to the available experimental variation of this parameter. These values of the Mn-Mn distance are far above the value of 3.6Å that, according to interaction curve, separates the regions of positive and negative pressure gradients of the Curie temperature for this group of systems. To verify the appearance of the non-monotonous behavior we extended the calculation to smaller values of the lattice constant corresponding to larger applied pressures. We compare empirical and calculated dependencies. The influence of the Mn-Ni atomic interchange on the magnetism of the system is also studied.

The paper is organized as follows. In Sec. II we present the calculational approach. Section III contains the results of the calculations and discussion. Section IV gives the conclusions.

II. CALCULATIONAL METHOD

The calculations are carried out with the augmented spherical waves method²⁰ within the atomic-sphere approximation.²¹ The exchange-correlation potential is chosen in the generalized gradient approximation.²² A dense Brillouin zone (BZ) sampling $30 \times 30 \times 30$ is used. To establish the relation between the lattice parameters and applied pressure we use the following expression ob-

tained experimentally in Ref.19

$$\frac{(V - V_0)}{V_0} = -aP + bP^2 \quad (1)$$

where $a = 8.64 \cdot 10^{-3} \text{GPa}^{-1}$, $b = 1.13 \cdot 10^{-4} \text{GPa}^{-2}$ and V_0 is the volume of the unit cell at the ambient pressure. The radii of all atomic spheres are chosen equal.

We describe the interatomic exchange interactions in terms of the classical Heisenberg Hamiltonian

$$H_{eff} = - \sum_{\mu, \nu} \sum_{\mathbf{R}, \mathbf{R}'} \underset{(\mu \mathbf{R} \neq \nu \mathbf{R}')}{J_{\mathbf{R}\mathbf{R}}^{\mu\nu}} \mathbf{s}_{\mathbf{R}}^{\mu} \mathbf{s}_{\mathbf{R}'}^{\nu} \quad (2)$$

In Eq.(2), the indices μ and ν number different sublattices and \mathbf{R} and \mathbf{R}' are the lattice vectors specifying the atoms within sublattices, $\mathbf{s}_{\mathbf{R}}^{\mu}$ is the unit vector pointing in the direction of the magnetic moment at site (μ, \mathbf{R}) . The systems considered contain three 3d atoms in the unit cell with positions shown in Fig.1.

We employ the frozen-magnon approach^{23,24,25} to calculate interatomic Heisenberg exchange parameters. The calculations involve few steps. In the first step, the exchange parameters between the atoms of a given sublattice μ are computed. The calculation is based on the evaluation of the energy of the frozen-magnon configurations defined by the following atomic polar and azimuthal angles

$$\theta_{\mathbf{R}}^{\mu} = \theta, \quad \phi_{\mathbf{R}}^{\mu} = \mathbf{q} \cdot \mathbf{R} + \phi^{\mu}. \quad (3)$$

The constant phase ϕ^{μ} is always chosen equal to zero. The magnetic moments of all other sublattices are kept parallel to the z axis. Within the Heisenberg model (2) the energy of such configuration takes the form²⁴

$$E^{\mu\mu}(\theta, \mathbf{q}) = E_0^{\mu\mu}(\theta) + \sin^2 \theta J^{\mu\mu}(\mathbf{q}) \quad (4)$$

where $E_0^{\mu\mu}$ does not depend on \mathbf{q} and the Fourier transform $J^{\mu\nu}(\mathbf{q})$ is defined by

$$J^{\mu\nu}(\mathbf{q}) = \sum_{\mathbf{R}} J_{0\mathbf{R}}^{\mu\nu} \exp(i\mathbf{q} \cdot \mathbf{R}). \quad (5)$$

In the case of $\nu = \mu$ the sum in Eq. (5) does not include $\mathbf{R} = 0$. Calculating $E^{\mu\mu}(\theta, \mathbf{q})$ for a regular \mathbf{q} -mesh in the Brillouin zone of the crystal and performing back Fourier transformation one gets exchange parameters $J_{0\mathbf{R}}^{\mu\mu}$ for sublattice μ .

The determination of the exchange interactions between the atoms of two different sublattices μ and ν is discussed in Ref. 26.

The Curie temperature is estimated within the mean-field approximation for a multi-sublattice material by solving the system of coupled equations^{26,27}

$$\langle s^{\mu} \rangle = \frac{2}{3k_B T} \sum_{\nu} J_0^{\mu\nu} \langle s^{\nu} \rangle \quad (6)$$

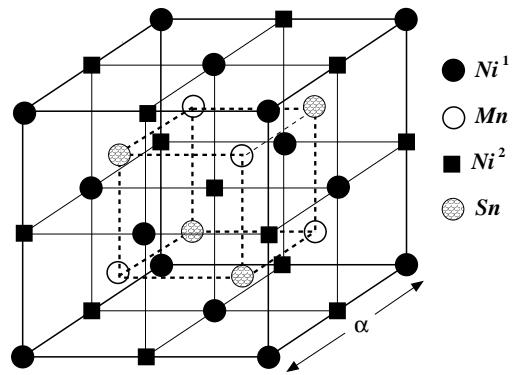


FIG. 1: Schematic representation of the $L2_1$ structure adapted by the full Heusler alloys. The lattice consists of four interpenetrating fcc sublattices with the positions $(0, 0, 0)$ and $(\frac{1}{2}, \frac{1}{2}, \frac{1}{2})$ for the Ni and $(\frac{1}{4}, \frac{1}{4}, \frac{1}{4})$ and $(\frac{3}{4}, \frac{3}{4}, \frac{3}{4})$ for the Mn and Sn, respectively.

TABLE I: Lattice parameters, magnetic moments and Curie temperatures in Ni_2MnSn at ambient pressure and applied pressure of 16 GPa. For comparison, the magnetic moment obtained with full potential FLAPW-GGA method is presented.

	$a=6.022 \text{ \AA} [P=0 \text{ GPa}]$	$a=5.821 \text{ \AA} [P=16 \text{ GPa}]$
Ni	0.21	0.19
Mn	3.73	3.47
Sn	-0.05	-0.05
Total	4.09, 4.10 ^a	3.81
T_c [calc]	362, 373 ^b	400
T_c [expt]	360 ^c , 342 ^d , 338 ^e	-

^aRef.35

^bRef.28

^cRef.40

^dRef.19

^eRef.36

where $\langle s^{\nu} \rangle$ is the average z component of $\mathbf{s}_{\mathbf{R}}^{\nu}$ and $J_0^{\mu\nu} \equiv \sum_{\mathbf{R}} J_{0\mathbf{R}}^{\mu\nu}$. Eq.(6) can be represented in the form of eigenvalue matrix problem

$$(\Theta - T\mathbf{I})\mathbf{S} = 0 \quad (7)$$

where $\Theta_{\mu\nu} = \frac{2}{3k_B} J_0^{\mu\nu}$, \mathbf{I} is a unit matrix and \mathbf{S} is the vector of $\langle s^{\nu} \rangle$. The largest eigenvalue of matrix Θ gives the value of Curie temperature.²⁷

III. RESULTS AND DISCUSSION

We will subdivide the discussion of the influence of the pressure on the electronic properties of Ni_2MnSn in two parts. First, we present a detailed study of the low-pressure region where an experimental information is available (We extend this interval up to ~ 20 GPa). In particular we verify the monotonous increase of the

Curie temperature with increasing pressure in this region. Then we consider a much larger interval of the variation of the lattice parameter to study the occurrence of the non-monotonous behavior of the Curie temperature.

A. Low pressure region

We begin with the discussion of the effect of pressure on the electronic structure. In Fig. 2, we compare the density of states calculated for the ambient pressure and the applied pressure of 16 GPa. As expected, the pressure leads to the broadening of the bands that stems from the decreasing inter-atomic distances and, therefore, increasing overlap of the atomic states. One of the consequences of the band broadening is the trend to the decrease of the magnetic moments. This trend is demonstrated in table I and Fig. 3. In Fig. 3 we present a detailed information on the atomic and total magnetic moments for the range of pressures up to 20.6 GPa. The dependence of the Mn magnetic moment on pressure can be well represented by a linear function with a negative slope. The behavior of the induced moment of Ni is more peculiar. The dependence deviates strongly from the straight line and shows weak oscillations in the high-pressure part of the curve. This behavior reflects the details of the pressure dependence of the band structure, in particular, the form of the DOS in the energy region close to the Fermi level and the character of the Mn-Ni hybridization. Since these weak oscillations do not play noticeable role in the issues we focus on in this paper we do not further investigate their origin. The induced moment on Sn has the direction opposite to the direction of the Mn moment. Its value decreases slowly with increasing pressure. The spin polarization at the Fermi level shows very weak pressure dependence.

Thus the decreasing lattice constant produces a clear trend to a monotonous decrease of the atomic magnetic moments. For our purpose of the investigation of the pressure dependence of the Curie temperature it is important to relate the increasing band width and decreasing magnetic moments to the properties of the inter-atomic exchange interactions.

In the spirit of the Heisenberg model of localized moments one expects that decreasing atomic moments produce the trend to the decrease of the inter-atomic exchange interactions by the factor of M_p^2/M_0^2 where M_p is the atomic moment at pressure P and M_0 is the moment at the ambient pressure. Correspondingly, one expects the trend to decreasing Curie temperature resulting from decreasing atomic moments.

An opposite monotonous trend to increasing inter-atomic exchange interactions is produced by increasing electron hopping and, as a result, more efficient mediation of the exchange interactions between magnetic atoms. The competition of two opposite trends opens possibility for both increase and decrease of the Curie temperature with applied pressure as well as for a non-

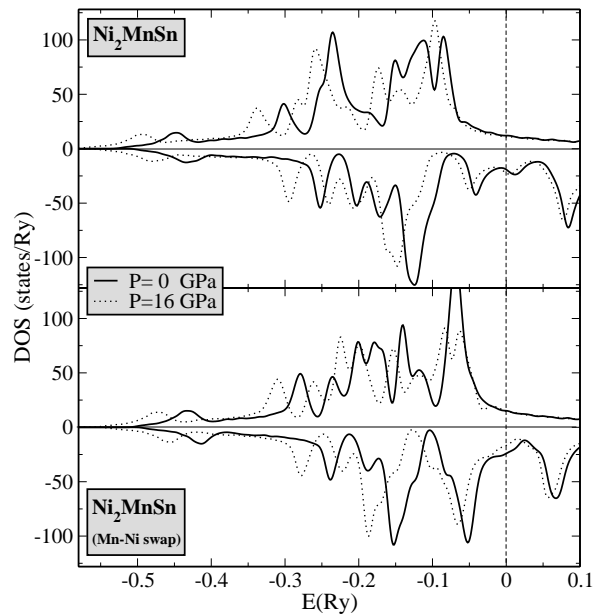


FIG. 2: Upper panel: Spin projected density of states of Ni_2MnSn for ambient pressure and applied pressure of 16 GPa. Lower panel: The same for the case of Mn-Ni atomic interchange.

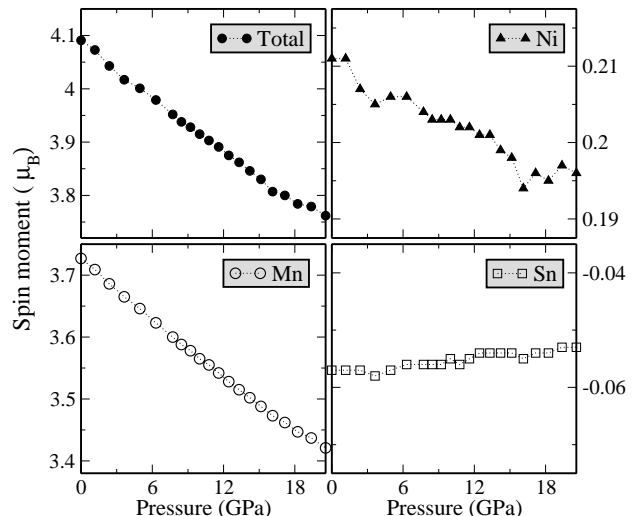


FIG. 3: Pressure dependence of magnetic moments in Ni_2MnSn .

monotonous pressure dependence in a larger pressure interval.

In Fig. 4a, we present the calculated inter-atomic exchange parameters of Ni_2MnSn for pressures of 0 and 16 GPa. For comparison, a zero-pressure result of previous calculation is also presented. At both pressures the patterns of inter-atomic exchange interactions are very similar. This similarity involves both Mn-Mn and Mn-Ni exchange interactions. The Mn-Mn interactions are

long-ranged reaching beyond the 8th nearest neighborhood distance and have the RKKY-type oscillating character. The inter-sublattice Mn–Ni interaction behaves very differently. A sizable interaction takes place only between nearest neighbors. Note that Fig.4a does not present all calculated exchange parameters: the exchange parameters have been evaluated up to the inter-atomic distances of $8.7a$ that corresponds to about 70 coordination spheres. The absolute value of the parameters decays quickly with increasing interatomic distance. In Fig. 4b, we demonstrate the convergence of the calculated Curie temperature with respect to increasing number of the atomic coordination spheres. The main contribution to T_c comes from the interaction between atoms lying closer than $3a$. After $5a$ no sizable contribution is detected.

In Fig.4a, we compare our exchange parameters for Ni_2MnSn at zero pressure with the exchange parameters calculated recently by Kurtulus *et al.*²⁸ Kurtulus *et al.* used TB-LMTO-ASA method and local spin-density approximation (LSDA). The inter-atomic exchange parameters were evaluated using the real-space approach by Liechtenstein *et al.*²⁹ This approach and the frozen-magnon technique employed in the present paper are equivalent to each other. In the real-space method by Liechtenstein *et al.* the inter-atomic exchange parameters are calculated directly whereas in the frozen-magnon approach they are obtained by the Fourier transformation of the magnon dispersion.

In Table I, we present the MFA estimation of the Curie temperature. It is in good agreement with available experimental values overestimating them somewhat. An overestimation of the Curie temperature is a usual feature of the MFA.^{30,31,32} It arises from the property that the MFA expression for T_c corresponds to an equal weighting of the low- and high-energy spin-wave excitations. A better weighting of the magnetic excitations is provided by the random-phase approximation (RPA).³² However, in the case of the lattices with high atomic coordination numbers and in the cases of the magnon dispersion deviating strongly from a simple sinusoidal form the both MFA and RPA can give similar values of the Curie temperature making the MFA estimation reliable.^{33,34} A good agreement of the theoretical and experimental T_c values shows that the MFA is well applicable for the given system.

The pressure dependence of the interatomic exchange parameters is presented in Fig. 5. The corresponding Curie temperature is shown in inset in Fig 8. The analysis shows that the leading contribution into Curie temperature is given by the Mn–Mn exchange interactions within the first three coordinations spheres. The numbers of the atoms in these spheres are 12, 6 and 24, respectively for the first, second and third spheres. The exchange parameters corresponding to the second and third coordination spheres increase monotonously with increasing pressure determining the increase of the Curie temperature (Fig 8). Thus, the increase of the exper-

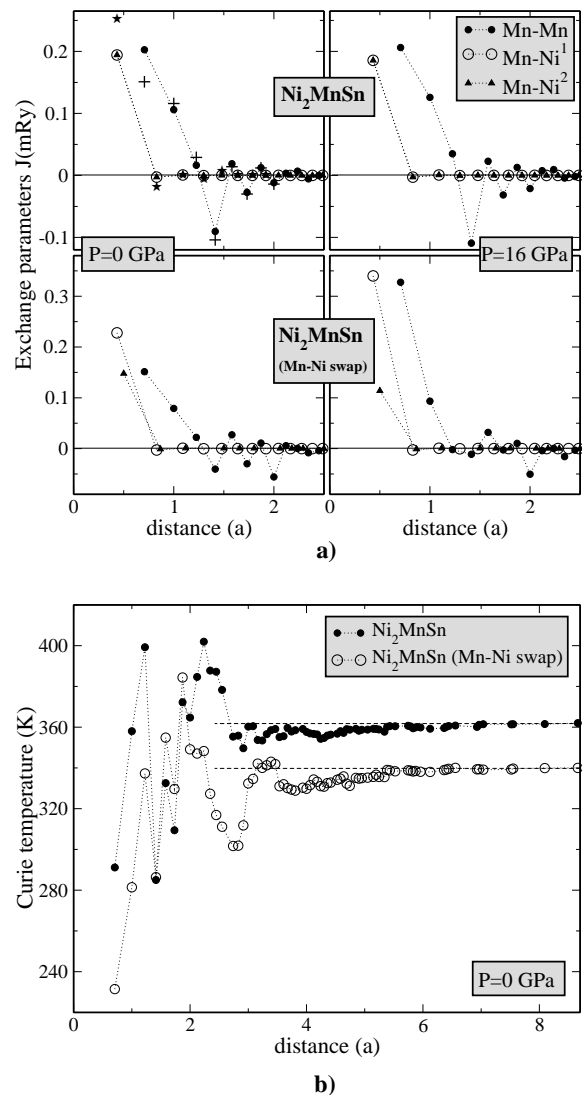


FIG. 4: a) Upper panel: Interatomic exchange parameters of Ni_2MnSn for ambient pressure and applied pressure of 16 GPa. Lower panel: The same for the case of Mn–Ni atomic interchange. Zero pressure comparison of both Mn–Mn (+) and Mn–Ni (*) exchange parameters with Ref.28 is also shown. b) Pressure variation of the Curie temperature with increasing number of coordination spheres with and without Mn–Ni atomic interchange.

imental Curie temperature with pressure in the corresponding pressure region¹⁹ is well confirmed by the calculations. In terms of the competition of the two opposite trends discussed above this result means a stronger effect of the increasing hopping compared with the effect of decreasing atomic moments. Such a behavior is expected for large inter-atomic distances.

Note that in the interval from 9 GPa to 16 GPa we obtain a flat feature in the pressure dependence of the Curie temperature. This behavior is in a correlation with the recent experiment of Kyuji *et al.*³⁶ who obtained the

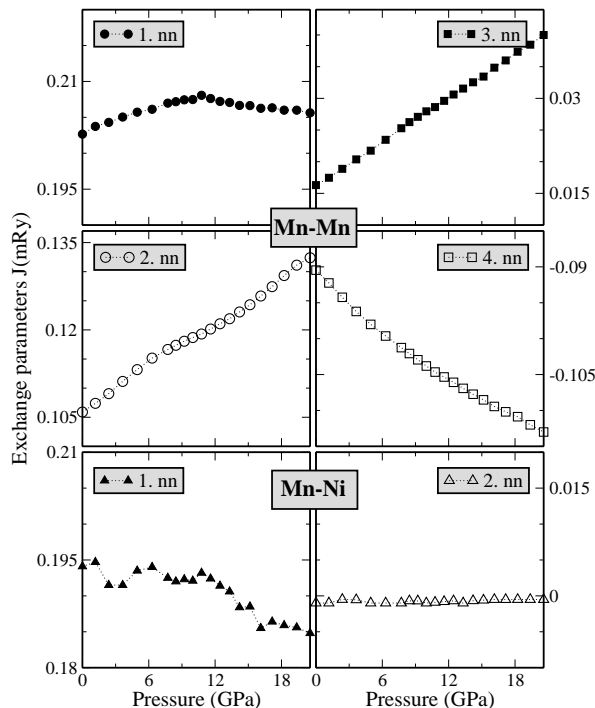


FIG. 5: Pressure dependence of the first four nearest neighbor Mn–Mn exchange parameters and two Mn–Ni exchange parameters.

Curie temperature increase from 338K at the ambient pressure to 395K at 12 GPa. At ~ 7 GPa they obtained a decrease of the pressure gradient that can be put into correspondence to the theoretical flat feature.

Both measured and calculated Curie temperatures are in good agreement with the empirical interaction curve for the corresponding region of the Mn–Mn distances (Fig. 8).

B. High pressure region

To verify the non-monotonous pressure dependence of T_c predicted by the interaction curve we extended the calculation to smaller Mn–Mn distances down to 3.09\AA . The calculated magnetic moments are presented in Fig. 6. The Mn moment decreases with the reduction of Mn–Mn distance. An interesting feature is obtained at $d_{Mn-Mn} = 3.416\text{\AA}$ where the value of the magnetic moment changes discontinuously. To study the origin of the discontinuity we employed the fixed-spin-moment method^{37,38,39} that allows the calculation of the total energy as a function of the spin moment for a given lattice parameter. The corresponding curves are presented in the inset in Fig. 6. For large Mn–Mn distance the curve has one minimum corresponding to a high-spin state. In the region of the discontinuity the curve has two local minima revealing the presence of a metastable state. At

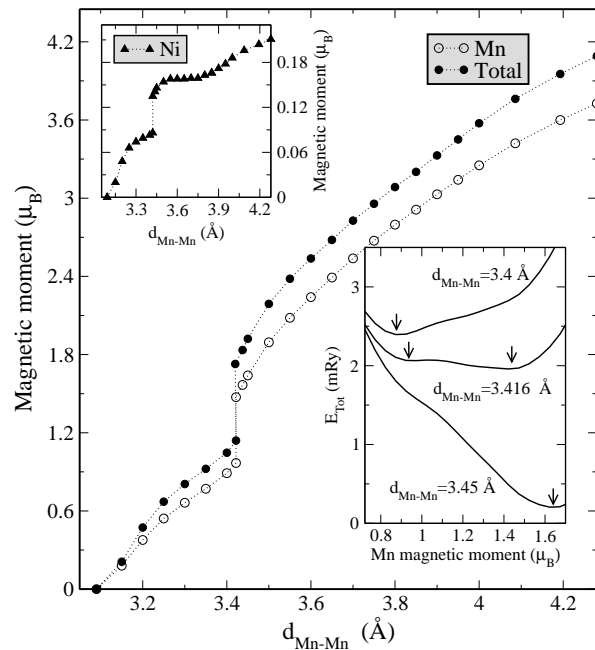


FIG. 6: Mn and total magnetic moments as a function of the Mn–Mn distance. Upper inset shows the variation of induced Ni moment with Mn–Mn distance. Lower inset shows E_{Tot} as a function of Mn magnetic moment for selected Mn–Mn interatomic distances. Arrows indicate the energy minima.

the point of discontinuity the minimum corresponding to the low-spin state becomes lower. With further decrease of the lattice volume the minimum corresponding to the high-spin state disappears. At $d_{Mn-Mn} = 3.09\text{\AA}$ the magnetic moment vanishes and the ground state of the system becomes a Pauli-paramagnet.

In Fig. 7, the first four nearest neighbor Mn–Mn exchange interactions are presented for the broad interval of the Mn–Mn interatomic distance. The pressure region discussed in the preceding section corresponds to the last three points in the plot. Three of the four leading parameters show nonmonotonous behavior that is reflected in the nonmonotonous behavior of the Curie temperature (Fig. 8). The absolute values of the 2nd, 3rd and 4th neighbor Mn–Mn parameters first increase with pressure, reach their maxima at the Mn–Mn distances in the region from about 4.0\AA to about 3.6\AA and decrease strongly with further decrease of the Mn–Mn distance. There are some weak peculiarities in the behavior of the exchange parameters at the region after the discontinues transition such as additional local extrema in the 1st, 3th and 4th neighbor parameters. They, however, compensate each other and the Curie temperature has only one maximum at the Mn–Mn distance of about 3.8\AA (Fig.8).

The non-monotonous behavior of the exchange parameters and T_c can be interpreted as a result of the competition of two opposite monotonous trends appearing with the variation of the Mn–Mn distances discussed in the previous section. In the low-pressure region the in-

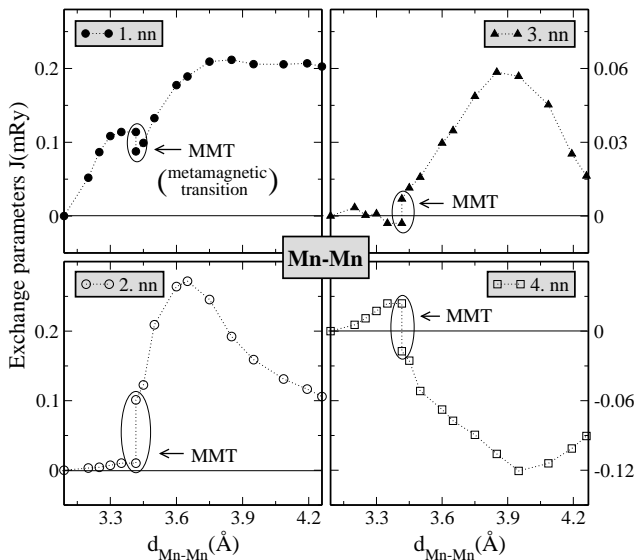


FIG. 7: The first four nearest neighbor Mn-Mn exchange interactions in Ni_2MnSn as function of Mn-Mn interatomic distance. The ellipses show the region of the metamagnetic transition.

fluence of the increasing hopping prevails while in the high-pressure region the influence of decreasing magnetic moments becomes more important.

Qualitatively, the calculated pressure dependence of T_c in the broad pressure interval is in agreement with the Kanomata's empirical interaction curve. Indeed, we obtained non-monotonous pressure dependence characterized by one maximum separating the regions of positive and negative pressure gradients. The low-pressure part of the calculated dependence is in reasonable quantitative agreement with the Kanomata's interaction curve. For smaller lattice volumes the calculated Curie temperature decreases faster than it is prognosticated by the interaction curve. The calculations predict the discontinuity in the pressure dependence of the Curie temperature of Ni_2MnSn which is absent in the empirical interaction curve. The extension of the measurements to higher pressures is desirable to verify the predictions of the calculations.

C. Atomic inter-sublattice interchange

The calculations of the Curie temperature of Ni_2MnSn discussed in the preceding sections are in good correlation with measured T_c values for the range of pressures studied experimentally. A detailed numerical comparison shows, however, that the theoretical pressure derivative, dT_c/dP , estimated as 3.22 K/GPa is substantially smaller than the experimental estimation of 7.44 K/GPa obtained by Gavriluk *et al.*¹⁹ To verify the role of the atomic interchange between Ni and Mn sublattices observed experimentally¹⁹ we performed calculation for a

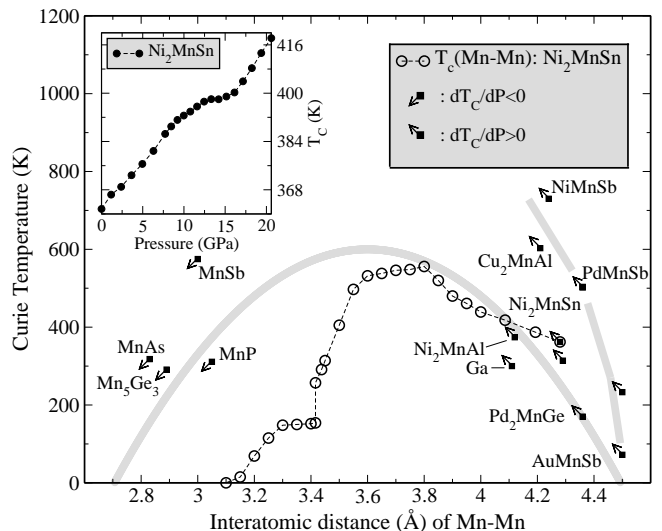


FIG. 8: Schematic representation of Kanomata's empirical interaction curve and the calculated Curie temperature as a function of the interatomic Mn-Mn distance in Ni_2MnSn . Inset shows pressure variation of T_c in the low pressure region. Small rectangles present the Curie temperatures of the corresponding compounds at ambient pressure. The attached arrows show the sign of dT_c/dP . (The experimental information is taken from Ref.40).

model system where the atoms of the Mn sublattice are interchanged with the atoms of one of the Ni sublattices. Although this model is a strong simplification of the experimental situation it allows the investigation of the trends resulting from the Mn-Ni interchange.

With Mn-Ni interchange we obtain a substantial difference in the electron structure of the system. The corresponding DOS and magnetic moments for ambient and applied pressure of 16 GPa are presented in Fig.2 and table II. In this case the Mn states hybridize differently with the states of two Ni atoms. As a result the magnetic moments of the Ni atoms assume different values. The total magnetic moment per formula unit decreases from $3.50\mu_B$ at ambient pressure to the $3.09\mu_B$ at the applied pressure of 16 GPa. The decrease of the total magnetic moment is mostly the result of the reduction of the Mn moment. Note that at the pressure of 16 GPa the relative variation of the total magnetic moment is two times larger than in Ni_2MnSn without Mn-Ni interchange. The change in the shape of the 3d peaks and broadening of the bands are similar to those for the system without swapping.

At zero pressure the pattern of exchange parameters (Fig. 4) and resulting Curie temperature (Table II) are very similar to the case without Mn-Ni interchange. However, the situation is different at applied pressure of 16 GPa. Both Mn-Mn and Mn-Ni¹ nearest-neighbor exchange parameters increase substantially. The remaining exchange parameters show small pressure dependencies. The interaction of the Mn moment with the moment of

TABLE II: Lattice parameters, magnetic moments and Curie temperatures at ambient pressure and applied pressure of 16 GPa for Ni₂MnSn with Mn–Ni atomic interchange.

	$a=6.022 \text{ \AA} [P=0 \text{ GPa}]$	$a=5.821 \text{ \AA} [P=16 \text{ GPa}]$
Ni ¹	0.21	0.26
Ni ²	0.08	0.05
Mn	3.24	2.80
Sn	-0.04	-0.03
Total	3.50	3.09
T _c	340	562

the second Ni atom is slightly reduced. The substantial increase of the leading exchange parameters with pressure results in considerable change of the Curie temperature from 400 K at ambient pressure to 562 K at 16 GPa. Assuming a linear variation of T_c with pressure we estimate the pressure derivative, dT_c/dP , as 12.5 K/GPa. This value of dT_c/dP exceeds strongly the corresponding value for the system without Mn–Ni atomic interchange. Since the number of the swapped Mn and Ni atoms in our model is much larger than in the samples measured the calculated dT_c/dP cannot be directly compared with the experimental pressure derivative. Important, however, that the Mn–Ni atomic interchange increases the pressure derivative of T_c that gives an explanation for the low value of the theoretical pressure derivative in the case of the system without swapping. A detailed study of the influence of the inter–sublattice atomic interchange on the electron properties of the Heusler systems is an interesting extension of the present study.

IV. CONCLUSION

In conclusion, we have systematically studied the pressure dependence of exchange interactions and Curie temperature in full Heusler alloy Ni₂MnSn within the parameter–free density functional theory. We show that the character of the pressure dependence of the exchange interactions is a consequence of the complex interplay of competing trends in the electronic properties of the system. In agreement with experiment, the Curie temperature increases with increasing pressure in the pressure region studied. Extending our theoretical study onto a larger pressure interval we obtained non–monotonous T_c dependence and the presence of the metamagnetic transition. The T_c behavior in the whole pressure interval is in qualitative correlation with the Kanomata’s empirical interaction curve. In the low–pressure region there is good quantitative agreement between calculated values and the prediction of the empirical rule. The Mn–Ni atomic interchange is shown to increase the pressure derivative of the Curie temperature that suggests the physical mechanism for the improved agreement between the experimental and theoretical estimations of this parameter.

Acknowledgments

The financial support of Bundesministerium für Bildung und Forschung is acknowledged.

-
- ¹ J.M. Leger, C. Loriers-Susse, and B. Vodar, Phys. Rev. B **6**, 4250 (1972).
 - ² A. Fujita and K. Fukamichi, M. Yamada and T. Goto, J. Appl. Phys. **93**, 7263 (2003).
 - ³ S. Wei, R. Duraj, R. Zach, M. Matsushita, A. Takahashi, H. Inoue, F. Ono, H. Maeta, A. Iwase and S. Endo, J. Phys.: Condens. Matter **14**, 11081 (2002).
 - ⁴ M. Nishino, N. Fujii, S. Endo, T. Kanomata and F. Ono, Phys. Lett. A, **276**, 133 (2000).
 - ⁵ H. Hasegawa and D. G. Pettifor, Phys. Rev. Lett., **50**, 130 (1983).
 - ⁶ Arti Kashyap, A. K. Solanki, T. Nautiyal, and S. Auluck, Phys. Rev. B, **52**, 13471 (1995).
 - ⁷ H. Yamada, K. Fukamichi and T. Goto, Rev. B, **65**, 024413 (2001).
 - ⁸ H. Yamada, K. Terao, K. Kondo and T. Goto, J. Phys.: Condens. Matter **14**, 11785 (2002).
 - ⁹ S. Morán, C. Ederer, and M. Fähnle, Phys. Rev. B **67**, 012407 (2003).
 - ¹⁰ J. Kuneš, Wei Ku. W. E. Pickett, cond–mat/0406229
 - ¹¹ L. Castellitz, A. Metallkde. **46**, 198 (1955).
 - ¹² H. Ido, T. Suziki and T. Kaneko, J. Phys. Soc. Japan, **29**, 1490 (1970).
 - ¹³ T. Kaneko, H. Yoshida, and K. Kamigaki, J. Appl. Phys. **52**, 2046 (1981).
 - ¹⁴ N. Menyuk, J.A. Kafalas, K. Dwight and J. B. Goodenough, Phys. Rev. **177**, 942 (1969).
 - ¹⁵ T. Kanomata, K. Shirakawa and T. Kaneko, J. Magn. Magn. Mater. **65**, 76 (1987).
 - ¹⁶ T. Kaneko, K. Shirakawa, T. Kanomata, K. Watanabe and H. Masumoto, J. Magn. Magn. Mater. **54**, 933 (1986).
 - ¹⁷ T. Kaneko, K. Watanabe, K. Shirakawa, and H. Masumoto, J. Magn. Magn. Mater. **31**, 79 (1983).
 - ¹⁸ K. Shirakawa, T. Kanomata and T. Kaneko, J. Magn. Magn. Mater. **70**, 421 (1987)
 - ¹⁹ A. G. Gavriluk, G. N. Stepanov, V. A. Sidorov and S. M. Irkaev, J. Appl Phys. **79**, 2609 (1995).
 - ²⁰ A. R. Williams, J. Kübler, and C. D. Gelatt, Phys. Rev. B **19**, 6094(1979).
 - ²¹ O. K. Andersen, Phys. Rev. B **12**, 3060 (1975).
 - ²² J. P. Perdew and Y. Wang, Phys. Rev. B **45**, 13244 (1992).
 - ²³ N. M. Rosengaard and B. Johansson, Phys. Rev. B **55** 14975 (1997).
 - ²⁴ S. V. Halilov, H. Eschrig, A. Ya. Perlov, and P. M. Oppeneer, Phys. Rev. B **58** 293 (1998).
 - ²⁵ L. M. Sandratskii and P. Bruno, Phys. Rev. B **67**, 214402 (2003).
 - ²⁶ E. Şaşıoğlu, L. M. Sandratskii and P. Bruno, Rev. B **70**, 024427 (2004).
 - ²⁷ P. W. Anderson, *Theory of magnetic exchange interac-*

- tions: *Exchange in insulators and semiconductors*, in *Solid State Physics*, Edited by F. Seitz and Turnbull (Academic Press, New York), Vol. 14 pp. 99-214.
- ²⁸ Y. Kurtulus, R. Dronskowski, G. D. Samolyuk, and V. P. Antropov, *Phys. Rev. B* **71**, 014425 (2005).
- ²⁹ A.I. Liechtenstein, M.I. Katsnelson, V.P. Antropov, and V.A. Gubanov, *J. Magn. Magn. Mater.* **67**, 65 (1987).
- ³⁰ R. F. Sabiryanov and S. S. Jaswal, *Phys. Rev. Lett.*, **79**, 155 (1997).
- ³¹ R. F. Sabiryanov and S. S. Jaswal, *J. Appl. Phys.* **81**, 5615 (1997).
- ³² M. Pajda, J. Kudrnovsky, I. Turek, V. Drchal, and P. Bruno, *Phys. Rev. B* **64**, 174402 (2001).
- ³³ G. Bouzerar, J. Kudrnovský, L. Bergqvist, and P. Bruno, *Phys. Rev. B* **68**, 081203(R) (2003).
- ³⁴ E. Şaşıoğlu, I. Galanakis, L. M. Sandratskii and P. Bruno, unpublished.
- ³⁵ Aniruddha Deb, N. Hiraoka, M. Itou, Y. Sakurai, M. Onodera and N. Sakai, *Phys. Rev. B* **63**, 205115 (2001).
- ³⁶ S. Kyuji, S. Endo, T. Kanomata and F. Ono, *Physica B* **237**, 523(1997).
- ³⁷ K. Schwarz and P. Mohn, *J. Phys. F: Met. Phys.* **14**, L129 (1984).
- ³⁸ P. H. Dederichs, S. Blügel, R. Zeller, and H. Akai, *Phys. Rev. Lett.*, **53**, 2512 (1983).
- ³⁹ L. M. Sandratskii and E. N. Kuvaldin, *J. Phys.: Condens. Matter* **3**, 7663 (1991).
- ⁴⁰ P. J. Webster and K. R. A. Ziebeck, in *Alloys and Compounds of d-Elements with Main Group Elements*, Part 2, edited by H. R. J. Wijn, Landolt-Börnstein, New Series, Group III, Vol. 19/c (Springer, Berlin, 1988), pp. 75-184.